Drug Design, Development and Therapy

Dovepress

open access to scientific and medical research

Open Access Full Text Article

ORIGINAL RESEARCH

Paeoniflorin Ameliorates BiPN by Reducing IL6 Levels and Regulating PARKIN-Mediated Mitochondrial Autophagy

Runjie Sun[1], Jiang Liu[2], Manya Yu[1], Mengting Xia[3], Yanyu Zhang[1], Xiaoqi Sun[1], Yunsheng Xu[4], Xing Cui[4]

[1]College of Traditional Chinese Medicine, Shandong University of Traditional Chinese Medicine, Jinan, 250014, People's Republic of China; [2]Department of Foreign Affairs Office, Affiliated Hospital of Shandong University of Traditional Chinese Medicine, Jinan, 250014, People's Republic of China; [3]First School of Clinical Medicine, Shandong University of Traditional Chinese Medicine, Jinan, 250014, People's Republic of China; [4]Second School of Clinical Medicine, the Second Affiliated Hospital of Shandong University of Traditional Chinese Medicine, Jinan, 250001, People's Republic of China

Correspondence: Yunsheng Xu; Xing Cui, Second School of Clinical Medicine, the Second Affiliated Hospital of Shandong University of Traditional Chinese Medicine, 1 Jingba Road, Jinan, 250001, People's Republic of China, Email xys65@126.com; cdz45@foxmail.com

Background: Bortezomib-induced peripheral neuropathy (BiPN) is a common complication of multiple myeloma (MM) treatment that seriously affects the quality of life of patients. The purpose of the present study was to explore the therapeutic effect of paeoniflorin on BiPN and its possible mechanism.

Methods: ELISA was used to measure the level of interleukin-6 (IL6) in the plasma of MM patients, and bioinformatics analysis was used to predict the mechanism underlying the effect of paeoniflorin on peripheral neuropathy. Cell and animal models of BiPN were constructed to evaluate mitochondrial function by measuring cell viability and mitochondrial quality and labeling mitochondria with MitoTracker Green. Nerve injury in mice with BiPN was assessed by behavioral tests, evaluation of motor nerve conduction velocity, hematoxylin-eosin (HE) staining, electron microscopy and analysis of the levels of reactive oxygen species (ROS). Western blotting and immunohistochemistry (IHC) were used to assess the expression of autophagy-related proteins.

Results: In MM patients, IL6 levels were positively correlated with the degree of PN. The results of bioinformatics analysis suggested that paeoniflorin ameliorated PN by altering inflammation levels and mitochondrial autophagy. Paeoniflorin increased PC12 cell viability and mitochondrial autophagy levels, alleviated mitochondrial damage, and reduced IL6 levels. In addition, paeoniflorin effectively improved the behavior of mice with BiPN, relieved sciatic nerve injury in mice, increased the expression of LC3II/I, beclin-1, and Parkin in sciatic nerve cells, and increased the expression of LC3B and Parkin in the nerve tissue.

Conclusion: The present study confirmed that paeoniflorin significantly ameliorated peripheral neuropathy (PN) caused by bortezomib, possibly by reducing IL6 levels to regulate PARKIN-mediated mitochondrial autophagy and mitochondrial damage.

Keywords: multiple myeloma, paeoniflorin, peripheral neuropathy, mitochondria, autophagy

Introduction

Multiple myeloma (MM) is a common hematological malignant tumor characterized by abnormal clonal proliferation and massive secretion of plasma cells in the bone marrow,[1] and MM accounts for more than 10% of all hematological malignancies.[2] The proteasome inhibitor bortezomib greatly improves the remission rate and survival rate of patients with MM and has become one of the main essential agents for antimyeloma treatment. Nevertheless, bortezomib has considerable neurotoxicity and can damage nerve fibers via many pathways, leading to the occurrence of bortezomib-induced peripheral neuropathy (BiPN).[3,4] The incidence rate of BiPN is approximately from 40% to 60%,[5] and the clinical manifestations mainly include pain, numbness, burning sensation in the limbs, and motor dysfunction.[6] Bortezomib neurotoxicity limits the clinical dosage and continuity of the treatment and seriously affects the application and efficacy of bortezomib. Unfortunately, exact etiology of BiPN has not been entirely elucidated, and there are no

Received: 7 April 2022
Accepted: 2 July 2022
Published: 13 July 2022

effective strategies to escape or treat BiPN.[7] Currently, the treatment of BiPN symptoms includes neuroprotective agents, such as vitamin B and methylcobalamin, which have poor clinical efficacy. Therefore, better strategies are urgently needed to alleviate BiPN.

Many studies have shown that proteasome inhibition can cause mitochondrial damage by inducing the accumulation of polyubiquitinated proteins, and mitochondrial dysfunction is the main factor that promotes the development and maintenance of PN.[8–10] Cavaletti et al[11] observed mitochondrial swelling in the sciatic nerve in a BiPN animal model. Bortezomib causes mitochondrial respiratory chain damage in the mitochondria, resulting in insufficient ATP production in the axons and occurrence of neuropathic pain.[12] Damaged mitochondria produce a large amount of reactive oxygen species (ROS), and the accumulation of ROS in the cells leads to further impairment of mitochondrial function and aggravation of peripheral nerve damage.[8,13] Hence, mitochondrial protection may be a promising therapeutic strategy for BiPN.

Recent studies have demonstrated that the immune response plays a vital role in the occurrence and development of neuropathic pain. Interleukin-6 (IL6) is the main mediator of the inflammatory response and is closely associated with chemotherapy-induced peripheral neuropathy (CIPN).[14,15] Yamamoto et al[3] detected elevated levels of proinflammatory cytokines (IL6, tumor necrosis factor alpha (TNF-α), and IL-1β) in the mouse models of BiPN. In addition, clinical studies detected significantly higher serum IL6 levels in MM patients after bortezomib treatment than that before the treatment, and patients with elevated IL6 levels present with varying degrees of neuropathy.[16,17] This observation suggests that IL6 is an independent risk factor for peripheral neuropathy (PN) in MM patients after bortezomib treatment.[18] Deficiency of Parkin and PINK1 can cause an impairment of mitochondrial autophagy, leading to the release of mitochondrial DNA (mtDNA) and triggering inflammation.[19–21] The Parkin and PINK1 pathways have been shown to be involved in mitochondrial autophagy. A number of recent studies demonstrated that IL6 influences the occurrence of certain diseases by interfering with PARKIN-mediated mitophagy. Tyrrell et al[22] confirmed that aging can lead to an increase in the levels of IL6 in cerebral blood vessels, thereby enhancing mitophagy through the PARKIN pathway and impairing mitochondrial function. Regarding neurological effects, IL6 has been shown to cause neuroinflammation in Parkinson's disease patients by interfering with PARKIN and PINK1-mediated mitophagy.[20]

Paeoniflorin is a biologically active compound purified from the Chinese herbal medicine plant *Paeonia lactiflora* and has been proven to induce a wide range of anti-inflammatory, pain-relieving, and immunomodulatory effects.[23] Furthermore, paeoniflorin is a potential neuroprotective agent. Paeoniflorin has been shown to reduce neuronal damage by decreasing the secretion of IL6 and other inflammatory factors or reducing the level of autophagy.[24–27] Unfortunately, alleviating effect of paeoniflorin on BiPN has been relatively rarely reported. Therefore, we designed the experiments to determine whether paeoniflorin can relieve BiPN by reducing IL6 levels to regulate PARKIN-mediated mitochondrial autophagy.

Materials and Methods

Clinical Data

Fifteen MM patients admitted to the Department of Hematology, Affiliated Hospital of Shandong University of Traditional Chinese Medicine were enrolled in the present study. All patients received bortezomib chemotherapy. The peripheral blood of the subjects was collected in a vacuum coagulation tube, and the plasma was obtained after centrifugation (10 min, 3000 rpm) and stored at −80°C. Enzyme-linked immunosorbent assay (ELISA) was used to measure IL6 levels in the plasma. The degree of BiPN was graded based on the system of the National Cancer Institute Common Toxicity Criteria for Adverse Events (NCI-CTCAE). The present study was conducted in accordance with the Helsinki Declaration revised in 2008, and informed consent was obtained from all participants.

Reagents and Instruments

PC12 pheochromocytoma cells were obtained from ATCC (Rockville, MD, USA), and paeoniflorin was purchased from Winherb Medical Science Co., Ltd. (purity: 98.96%, 23180-57-6, Shanghai, China). Bortezomib was purchased from Meilun Biotechnology Co., Ltd. (MB1040, Dalian, China), and a Cell Counting Kit-8 (CCK-8) was purchased from Servicebio Technology Co., Ltd. (G4103, Wuhan, China). An apoptosis kit was obtained from Keygen Biotech Co., Ltd. (KGA108, Nanjing, China), and a living cell mitochondrial damage/oxidation (NAO) fluorescence assay kit was from GenMed

(GMS10017.1, USA). Antibodies against LC3, p62, Beclin-1, Pink1, and Parkin were purchased from Santa Cruz Biotechnology (USA). An intelligent hot plate was obtained from Zhenghua Biologic Apparatus Facilities (ZH-YLS-6BS, Anhui, China), and a Sting thermal imager was obtained from Taimeng Software Co., Ltd. (PL-200, Chengdu, China). A multichannel physiological recorder was obtained from Biopac (MP160, USA), and a monoamine oxidase activity colorimetric assay kit (GMS50022.1) and purified mitochondrial cytochrome c oxidase activity assay kit (GMS10014.2) were purchased from GenMed (Shanghai, China).

Identification of Paeoniflorin and PN Targets and Pathway Enrichment Analysis

The PharmMapper, TCMSP, PubChem, and BATMAN-TCM databases were used to predict paeoniflorin targets. PN-related target genes were identified by the searches of the GeneCards and TTD databases using peripheral neuropathy as the keyword. The intersecting targets were selected, and a Venn diagram was generated. The IDs of obtained targets were converted into the UniProt IDs and were used to build a "paeoniflorin-target-disease" interactive network using Cytoscape 3.7.2. Gene Ontology (GO) and Kyoto Encyclopedia of Genes and Genomes (KEGG) pathway enrichment analyses of the targets were carried out using Metascape.

PC12 Cell Culture and Treatments

PC12 pheochromocytoma cells were incubated in RPMI-1640 medium containing 2 mM L-glutamine, 10 mM HEPES, 1 mM sodium pyruvate, 4500 mg/L glucose, 1500 mg/L sodium bicarbonate, streptomycin (100 μg/mL), penicillin (100 U/mL), 5% fetal bovine serum (FBS), and 10% heat-inactivated horse serum. PC12 cells were plated in collagen IV-coated 6-well culture plates at a density of 2×10^6 cells/well in the medium. After 10 days, PC12 cells differentiated into the neurons. The cells were divided into the control group (untreated neurons), model group (50 nM bortezomib), paeoniflorin low-dose group (50 nM bortezomib + 10 μM paeoniflorin), paeoniflorin medium-dose group (50 nM bortezomib + 20 μM paeoniflorin), and paeoniflorin high-dose group (50 nM bortezomib + 40 μM paeoniflorin) and collected after 24 h of incubation.

Assessment of Cell Viability

The effect of paeoniflorin on PC12 cell proliferation was assessed using the CCK-8 assay. PC12 cells were seeded in 96-well plates (100 μL per well) at a density of 5×10^3 cells/well. The cells of various groups were incubated at 37°C and 5% CO_2 for 12 h. Subsequently, 10 μL of CCK-8 solution was added to each well. After 2 h of incubation, the absorbance of each well was measured by a microplate reader at a wavelength of 450 nm, and each group was tested three times.

Determination of Mitochondrial Mass

We measured the mitochondrial mass using 10-nonyl bromide acridine orange (NAO). Mitochondria from PC12 cells were stained by NAO according to the protocol provided by Molecular Probes, and the staining was analyzed by flow cytometry.

Kinetics of Mitochondrial Lysis in vitro

Mitochondria were extracted from 3 various treatment groups, and the concentrations of monoamine oxidase (MAO) and cyclooxygenase (COX), which were used as biomarkers of mitochondrial membrane lysis, were measured. Analysis of the peaks of the mitochondrial membrane integrity as a function of time-dependent changes in the concentrations of matrix-specific enzymes was used to assess the trends in mitochondrial membrane lysis.

Determination of ATP, ADP, and AMP Concentrations in vitro

Perchloric acid and high-performance liquid chromatography (HPLC) were used to determine ATP, ADP, and AMP levels. PC12 cells were lysed in 50% perchloric acid and then centrifuged (at 4°C and 12,000 rpm for 30 min). The supernatant was transferred to a new centrifuge tube, and 2.5 M K_2CO_3 was added; the solution was centrifuged under the same conditions, and the supernatant was immediately analyzed by HPLC under the following conditions: a Hypersil

C18 5 μ analytical column; column length: 250 mm; column diameter: 4.6 mm; mobile phase: 0.005 M H_2PO_4 (pH 6.0); and UV detection at 254 nm. The results are expressed as μg/g protein.

Colocalization of the Mitochondria with Mitophagy Markers

PC12 cells were transfected with a mixture of 2 μg of the GFP-LC3 plasmid (Addgene, #22405) and 5 μL of Cell Light™ mitochondria-RFP (Thermo Fisher Scientific, C10505), and the colocalization of the LC3 puncta and mitochondria was examined using a laser scanning confocal microscope. The cells were stained with MitoTracker Green (Thermo Fisher Scientific, M7514), and then LysoTracker Red (Thermo Fisher Scientific, L-7528) was added to a final concentration of 25 nM. The number of the yellow puncta, which indicated the colocalization of the mitochondria with autophagosomes or lysosomes, was quantified using a confocal microscope. MitoTracker™ Red CMXRos (500 nM, Thermo Fisher Scientific, M7512) was added to the cells to label the mitochondria. The cells were incubated with a Parkin antibody (1:100) at 4°C overnight. After incubation with a secondary antibody, the cells were imaged using a fluorescence microscope at a wavelength of 550 nm for the detection of MitoTracker™ Red CMXRos and at appropriate wavelengths for the detection of fluorophore-conjugated secondary antibodies. The intensity of immunofluorescence staining was evaluated using ImageJ software.

Western Blotting

The cells were lysed using RIPA lysis buffer (Sparkjade, Jinan, China), and the protein concentration was measured using a bicinchoninic acid (BCA) protein assay kit (Beyotime, Shanghai, China). Equal amounts of sample protein were separated by 10% SDS–PAGE and transferred onto the polyvinylidene difluoride (PVDF) membranes (Sparkjade). The membranes were blocked with 5% skimmed milk at room temperature for 2 h and then incubated with anti-Tim23, anti-LC2II/I, anti-p62, anti-Parkin, or anti-Beclin-1 (Abcam) antibodies overnight at 4°C. After washing with PBS 3 times, a diluted secondary antibody was added, and the membrane was incubated at room temperature for 1 h. Then, the membrane was washed 3 times with PBS. Finally, a FluorChem Q imaging analysis system (Alpha Innotech) was used to detect the bands. The relative protein levels of Tim23, LC2II/I, p62, Parkin, and Beclin-1 were normalized to the level of GAPDH.

Animals and Treatments

A total of 45 8-week-old female C57BL/6J mice (weighing 18–20 g) were purchased from Beijing Vital River Laboratory Animal Technology Co., Ltd. (Beijing, China). All animal experiments were performed according to the protocols approved by the Animal Care Committee of Shandong University of Traditional Chinese Medicine (no: SDUTCM20201019001) following the Guidelines for the Care and Use of Laboratory Animals for Research Purposes. Thirty mice were randomly selected and administered bortezomib (1 mg/kg; days 1, 4, 8, and 11) by intraperitoneal injection to generate a BiPN model, and remaining 15 mice were automatically entered into the normal control group. Then, BiPN model mice were randomly divided into the model control group (15) and paeoniflorin group (15). Mice in the paeoniflorin group were treated with paeoniflorin solution (50 mg/kg/d) by gavage for 25 days.

Behavioral Testing

Mice were randomly selected from each group for behavioral tests on each experimental day, and all tests were performed between 8 am and 4 pm by researchers who were blinded to the animal group assignment.

Cold Plate Test

According to the method provided by Toyama et al,[28] hypersensitivity to a nonnoxious cold stimulus was assessed by counting the number of forepaw-shaking behaviors exhibited by mice placed on a cold plate at 15°C over a test period of 2.5 min. Each mouse was tested three times within an interval of 15 min, and the average value for each group of mice was calculated.

Hot Plate Test

According to the method described by Pascal Vachon[29] with slight modifications, the animals were gently placed on a hot plate at a temperature of 55 ± 0.5°C. The latency to the first hind paw lick or withdrawal was determined as a nociceptive threshold. The cutoff time was set to 1 min to avoid damage to the paw. Each mouse was tested 3 times with an interval of at least 15 min between the tests.

Thermal Paw Withdrawal Latency

According to the method described by Duggett et al[30] and slightly modified according to the instructions for experimental equipment, a light beam (light intensity: 25%) was applied to the center of each hind paw, and the latency from the start of stimulation to paw withdrawal was recorded. The test was performed three times in a noncontinuous manner to avoid sensitization. The timer was stopped when the mouse clearly tried to escape or licked its paw.

Motor Nerve Conduction Velocity

Mice anesthetized with chloral hydrate were placed on a heated pad in a room maintained at 25°C to ensure a constant rectal temperature of 37°C. The motor nerve conduction velocity (MNCV) between the sciatic notch and ankle was determined using a multichannel physiological recorder. Briefly, the proximal end of the sciatic nerve was stimulated with square wave pulses (duration: 0.01 ms, intensity: 1 V) delivered through the bipolar recording electrodes. The MNCV was calculated as follows: MNCV (m/s) = (distance between the stimulating and recording electrodes) /latency. The present study used the method of Walsh et al, and the method partly reproduced the description provided by the authors.[31,32]

Histological Analysis

Hematoxylin-Eosin (HE) Staining

The mouse sciatic nerve was removed, dehydrated, embedded in paraffin, and sectioned, and the sections were stained with HE. Nerve growth in mice of each group was detected using a microscope.

Transmission Electron Microscopy

After fixing, rinsing, and dehydration, the sciatic nerve was infused with EP812 embedding agent overnight and then stained with uranium and lead. The ultrastructure of the sciatic nerve was detected by an electron microscope, and the axon myelination ratio (the percentage of myelinated axons relative to the total number of axons) and g ratio (axon diameter/nerve fiber diameter) were calculated.

ROS Staining

According to the manufacturer's instructions, nerve cells were harvested and washed three times with 1 mL of PBS. The fluorescent probe 2',7'–dichlorofluorescin diacetate (DCFDA) was added, and the cells were incubated at 37°C for 30 min. A fluorescence microplate reader was used to measure the fluorescence signal values (excitation wavelength: 488 nm; emission wavelength: 525 nm).

Immunohistochemistry (IHC)

Neural tissue sections were fixed with 10% formaldehyde, destained, embedded in paraffin, sectioned, and subjected to antigen retrieval in a pressure cooker. The sections were cooled and incubated in 3% H_2O_2 for 10 min; the samples were treated with goat serum for 20 min and with primary antibodies against LC3B and Parkin (Affinity Biosciences, Cincinnati, OH, USA) for 1 h at 37°C. After washing with PBS, the sections were incubated with a secondary antibody for 30 min at room temperature and then with 3,3'-diaminobenzidine (DAB) substrate solution for 5 min. The sections were thoroughly washed, counterstained with hematoxylin, dehydrated in absolute ethanol, cleared in xylene, and imaged using a microscope.

Statistical Analysis

The experimental results were statistically analyzed using SPSS 26.0 and GraphPad Prism 9.0. Quantitative data with a normal distribution and homogeneity of variance are presented as the mean ± standard deviation. The differences

between two groups were assessed by Student's *t*-test, and the differences between multiple groups were evaluated by one-way ANOVA. Receiver operating characteristic (ROC) curves were used to determine the specificity of disease-related indicators. Statistically significant changes were classified as significant (*) at P<0.05 and very significant (**) at P<0.01.

Results

The Level of IL6 in the Plasma and the Progression of BiPN

We analyzed the serum IL6 levels and BiPN grade of 15 MM patients treated with bortezomib (12 cases with PN and 3 cases without PN). The data indicated that patients with PN (PN-positive group, PN grade ≥ 1) had higher plasma levels of IL6 than patients without PN (PN-negative group, PN grade = 0), and the difference was statistically significant (P ≤ 0.01) (Figure 1A). In addition, patients with a high PN grade also had higher expression levels of IL6, indicating that bortezomib-treated patients with high plasma IL6 levels had a greater risk of PN (Figure 1B).

Prediction of the Potential Mechanism Underlying the Effect of Paeoniflorin on PN

Network pharmacology was used to explore the mechanism underlying the therapeutic effect of paeoniflorin on PN. First, we confirmed 283 targets of paeoniflorin using the TCMSP, PubChem, BATMAN-TCM, and PharmMapper databases. Second, 807 PN-related genes were identified using the GeneCards and TTD databases. Subsequently, 41 intersecting genes were identified using a Venn diagram (Figure 2A). The STRING database was used to construct a protein–protein interaction (PPI) network of the common targets, and this PPI network was imported into Cytoscape 3.2.1 software to analyze the targets (Figure 2B and C). TNF, TP53, AKT1, and IL6 were identified as closely related to the therapeutic effect of paeoniflorin on PN. Metascape was used to perform GO and KEGG analyses to determine the potential mechanisms by which paeoniflorin influences PN. The targets were found to be significantly involved in the formation of neuronal receptors and cells, which is directly related to the generation of nerve cells. Moreover, according to the enriched biological process (BP) GO terms, paeoniflorin may be able to regulate neural-related proliferation and autophagy-related and inflammation biological processes, such as "regulation of glial cell proliferation", "neuroinflammatory response", "cellular response to interleukin-6", and "regulation of autophagy", to influence the growth of nerve cells (Figure 2D). The results of KEGG signaling pathway analysis are shown in Figure 2E. The most enriched pathways were closely related to peripheral neuropathy, such as "TNF signaling pathway", "HIF-1 signaling pathway", "apoptosis", "neurotrophin signaling pathway", "PI3K-Akt signaling pathway", and "regulation of autophagy". These findings

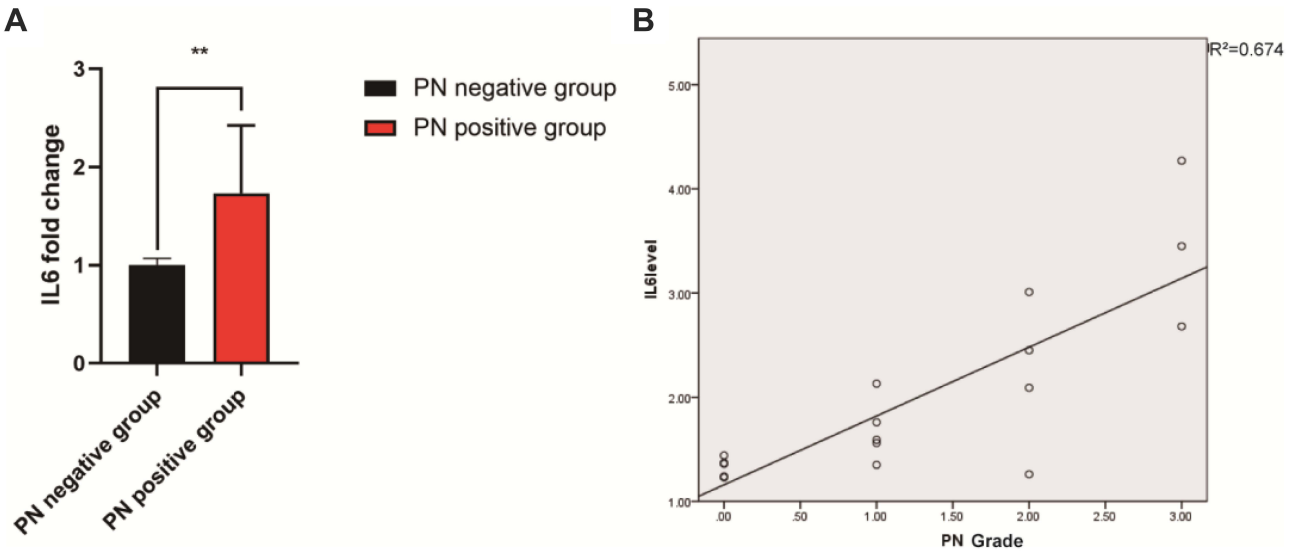

Figure 1 IL6 levels in multiple myeloma patients treated with bortezomib. (**A**) The expression level of IL6 was significantly higher in the PN-positive group than that in the PN-negative group. (**B**) The IL6 level was positively correlated with the BiPN grade (R^2=0.674). **P<0.01.

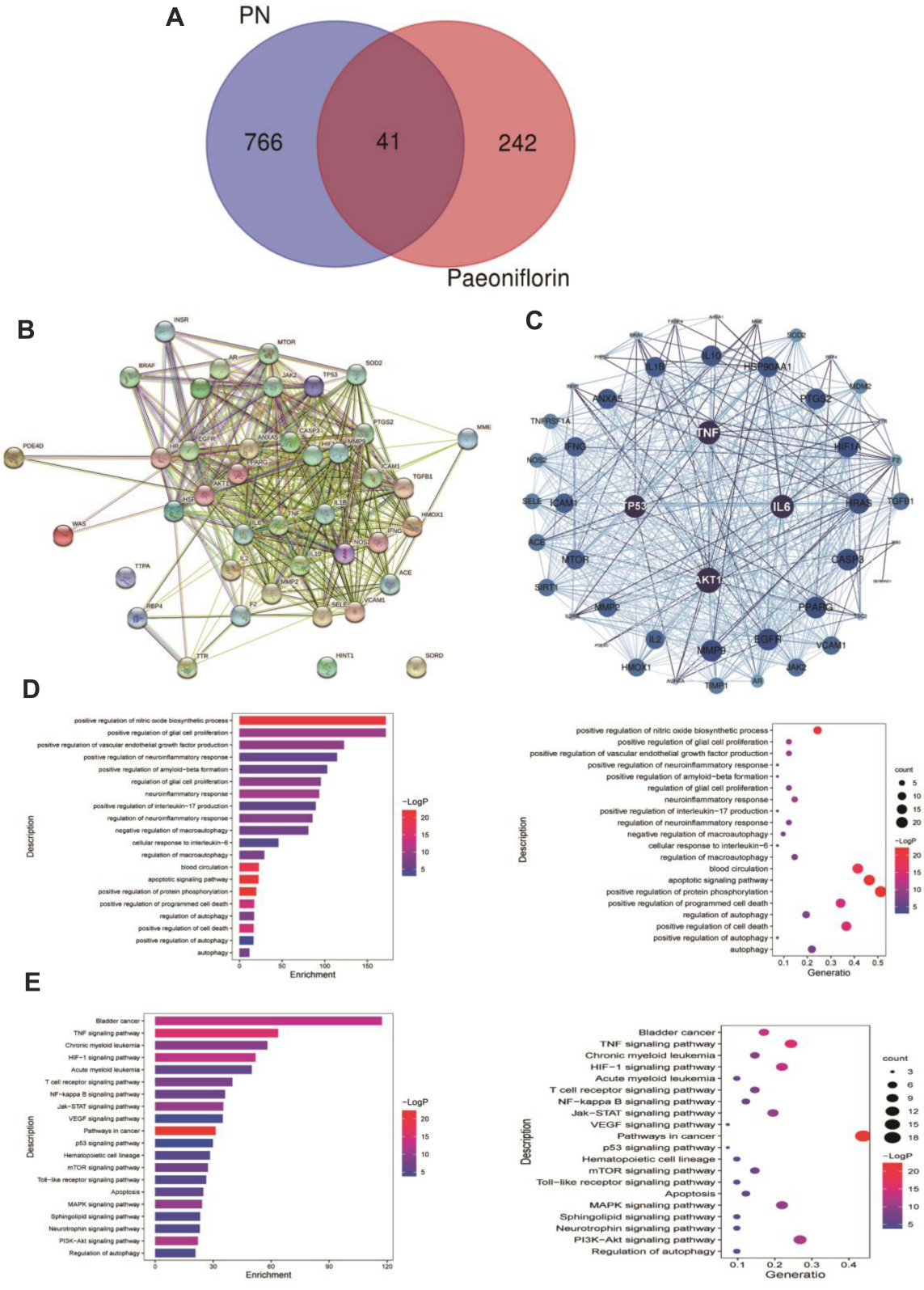

Figure 2 Prediction of a potential mechanism underlying the effect of paeoniflorin on peripheral neuropathy. (**A**) Venn diagram of the intersecting targets of paeoniflorin and PN. (**B**) Network diagram of the intersecting targets of paeoniflorin and PN. (**C**) IL6, AKT1, TP53, and TNF were considered core targets. (**D**) The top 20 enriched biological process terms according to GO enrichment analysis. (**E**) The top 20 signaling pathways enriched according to KEGG pathway analysis.

indicated that the pathological features of peripheral neuropathy are complex and that paeoniflorin has a potential to treat peripheral neuropathy.

Effects of Paeoniflorin on Cell Viability

To determine whether paeoniflorin alleviates nerve cell damage caused by bortezomib, the CCK-8 assay was used to measure the viability of various groups of the cells. The results showed that the activity of PC12 cells was significantly reduced after bortezomib treatment ($P<0.01$). Comparison with the model group at 24 h indicated that the viability of the cells of the paeoniflorin medium-dose group was significantly increased ($p<0.05$), and at 36 h and 48 h, the viability was significantly enhanced in all three paeoniflorin dose groups ($P<0.05$). In particular, 20 μM paeoniflorin induced the most significant improvement in the viability of PC12 cells treated with bortezomib (Figure 3A). Therefore, we used paeoniflorin at a dose of 20 μM as the treatment group for subsequent in vitro experiments. After treatment with bortezomib, the level of IL6 in the cells was significantly increased, and the level of IL6 was significantly decreased after treatment with paeoniflorin (Figure 3B).

Effects of Paeoniflorin on the Quality and Energy of the Mitochondria

NAO has been extensively used to measure the mitochondrial content in the cells. A decrease in NAO fluorescence intensity often indicates a decrease in mitochondrial quality.[33] We performed NAO staining using three groups of the cells; the results indicated that the NAO fluorescence intensity of bortezomib-treated PC12 cells (model group) was significantly reduced compared with that of control cells ($P<0.01$). However, the NAO fluorescence intensity of paeoniflorin-treated cells was significantly higher than that of the cells in the model group ($P<0.01$) (Figure 3C). This result indicated that paeoniflorin significantly reduced the damage to PC12 cell mitochondria caused by bortezomib. The activity levels of MAO and COX are mainly used to assess the mitochondrial function and oxidative stress damage. Comparison with the control group indicated that COX activity in the model group was significantly reduced at 12 h, 24 h, and 48 h, and MAO activity was significantly increased ($P<0.01$). However, COX activity in the cells treated with paeoniflorin was significantly higher than that in the model group at 12 h, 24 h, and 48 h, and MAO activity was significantly lower in the paeoniflorin -treated group than that in the model group ($P<0.01$). Therefore, complete cleavage of the mitochondrial contents in the cells was significantly delayed after the addition of paeoniflorin (Figure 3D and E). ATP is the energy source of biological organisms and plays an important role in cell metabolism. The levels of ADP, ATP, and AMP reflect the level of energy metabolism.[34] The results of the present study showed that compared with the corresponding values in the control group, the intracellular ATP and ADP levels in the model and treated group were significantly reduced at 12 h, 24 h, and 48 h ($P<0.01$), and the AMP content was significantly increased ($P<0.01$). In addition, comparison with the model group indicated that the contents of ATP and ADP in the treated group were significantly increased at 12 h, 24 h, and 48 h ($P<0.01$), and the content of AMP was significantly decreased ($P<0.01$) (Figure 3F–H). In addition, the number of the mitochondria in PC12 cells was significantly reduced by bortezomib treatment, and the number of the mitochondria in the treated group was significantly higher than that in the model group ($P<0.01$) (Figure 3I). These results indicated that paeoniflorin alleviated energy imbalance and mitochondrial damage caused by bortezomib.

Effects of Paeoniflorin on Mitochondrial Autophagy in PC12 Cells

We treated PC12 cells with bortezomib (model group) or paeoniflorin in combination with bortezomib (treated group) and investigated the level of mitophagy. As shown in Figure 4A, the intensity of GFP-LC3 fluorescence was decreased in the model group compared to that in the other groups; the number of LC3-positive cells in the model group was markedly decreased compared with that in the control group ($P<0.01$). Paeoniflorin significantly increased the fluorescence intensity of LC3. Moreover, as shown in Figure 4B, the relative number of the mitochondria was significantly decreased in PC12 cells treated with bortezomib compared with that in the control and treated groups ($P<0.01$).

The colocalization of the mitochondria (labeled with MitoTracker Red) and LC3 puncta (labeled with LC3 (green)) was detected using confocal fluorescence microscopy to confirm the mitophagy-promoting effect of paeoniflorin. The number of the mitochondria-localized LC3 puncta in bortezomib-treated cells was lower than that in control cells

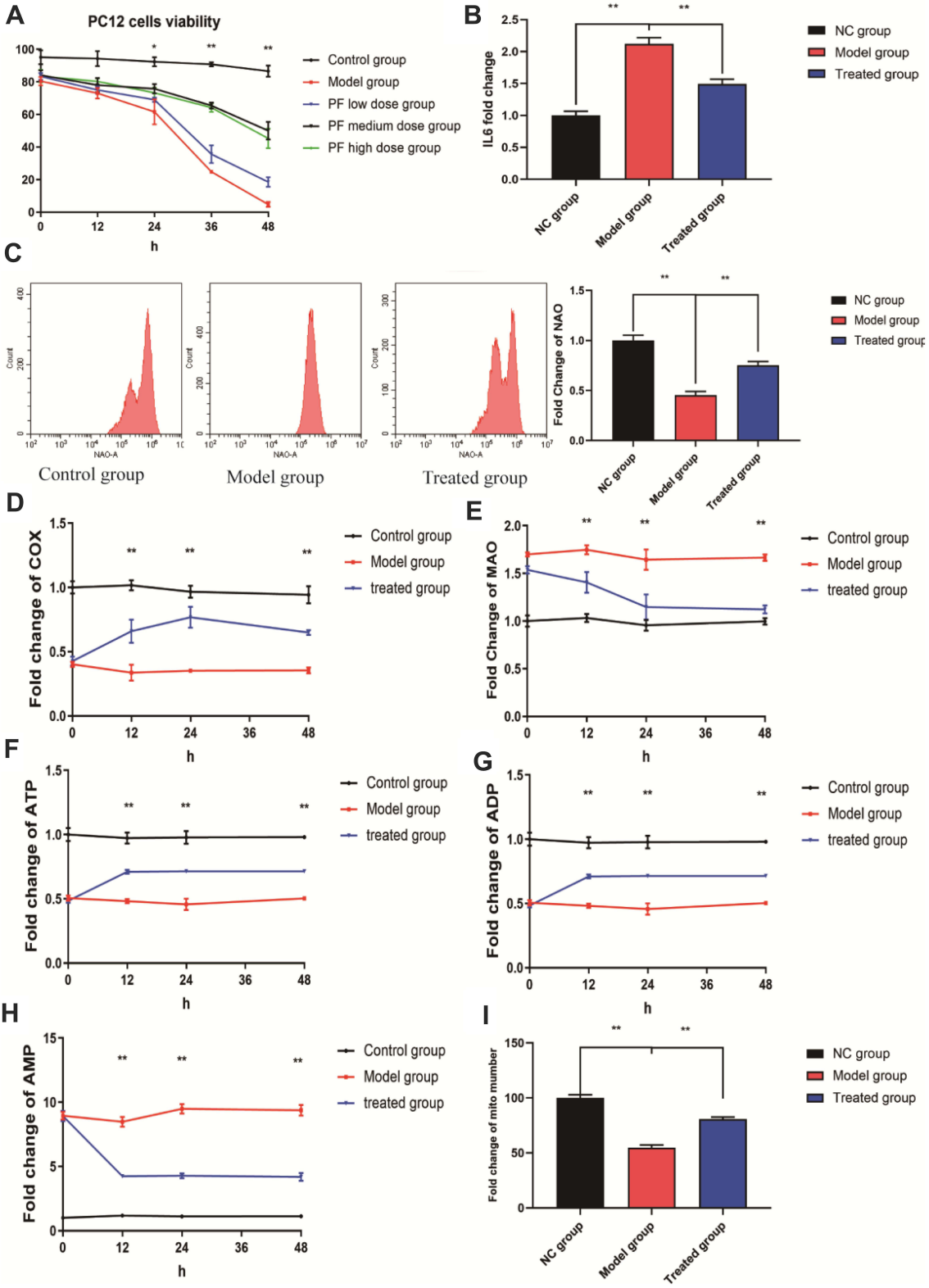

Figure 3 Effects of paeoniflorin on PC12 cells treated with bortezomib. (**A**) Paeoniflorin significantly increased the activity of PC12 cells after bortezomib treatment. (**B**) Paeoniflorin significantly reduced the level of IL6 in PC12 cells after bortezomib treatment. (**C**) Paeoniflorin significantly increased the NAO fluorescence intensity in the cells treated with bortezomib. (**D** and **E**) The levels of MAO and COX in PC12 cells were measured as markers of the outer and inner membrane kinase activity. COX activity in the paeoniflorin treatment group was significantly higher than that in the bortezomib group at 12 h, 24 h, and 48 h, and MAO activity was significantly reduced. (**F**–**H**) The ATP/ADP/AMP levels in various groups. (**I**) The number of the mitochondria in various groups. Each experiment was performed in triplicate. The data are presented as the mean±SD. *P<0.05 and **P<0.01.

https://doi.org/10.2147/DDDT.S369111 DovePress

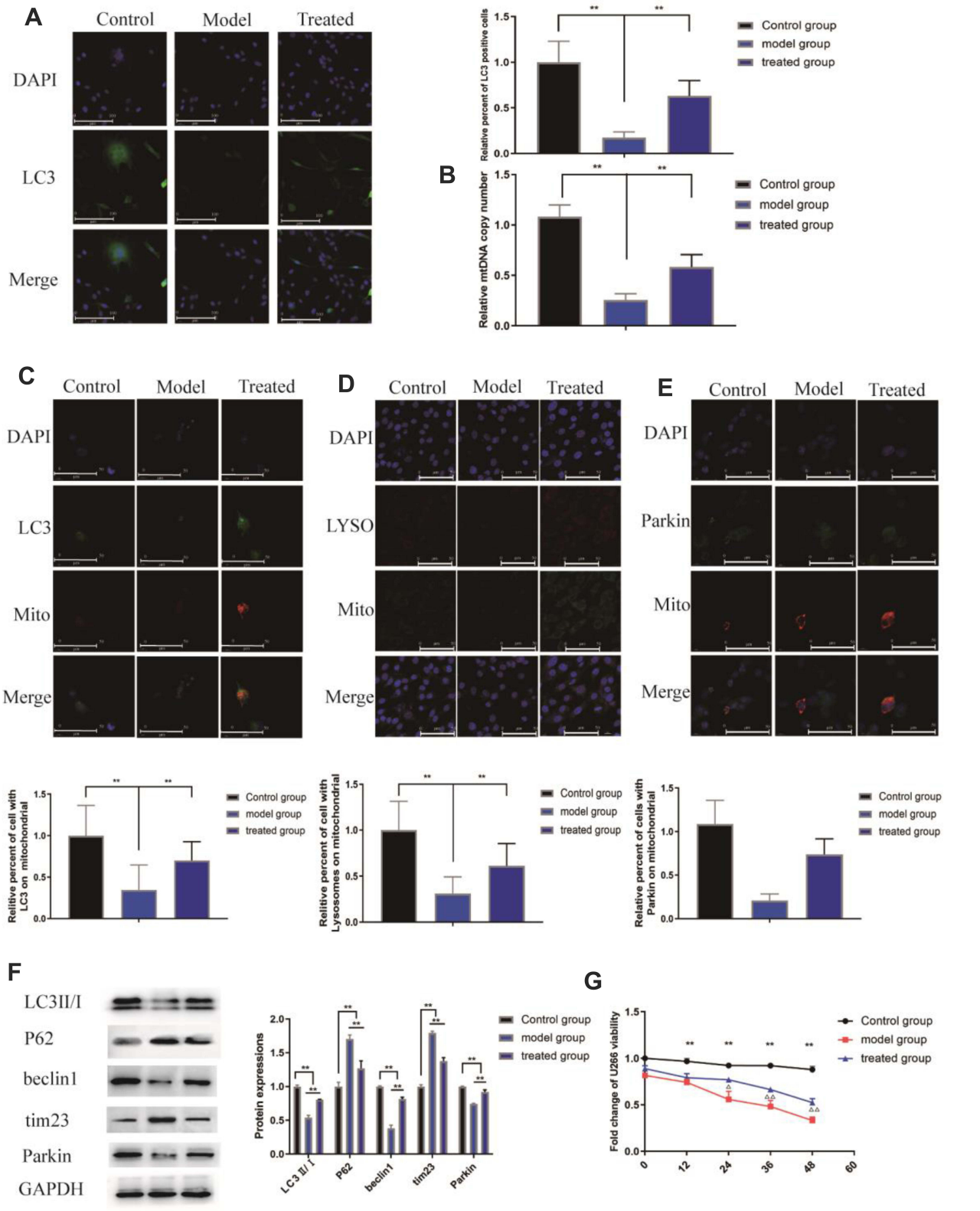

Figure 4 Effects of paeoniflorin on the level of mitophagy in PC12 cells treated with bortezomib. (**A**) The fluorescence intensity was evaluated using fluorescence microscopy; green indicates LC3, and DAPI was used to stain the nuclei. Paeoniflorin increased the LC3 fluorescence intensity. (**B**) Quantification of the mtDNA copy number in various groups. (**C**) Colocalization of the mitochondria and LC3 in various groups. Green represents LC3, and red represents the mitochondria. (**D**) Colocalization of the mitochondria and lysosomes in various groups. Red represents the lysosomes, and green represents the mitochondria. (**E**) Colocalization of mitochondria and Parkin in various groups. Green represents Parkin, and red represents mitochondria. (**F**) WB analysis of the protein levels of PARKIN, p62, Tim23, and LC3II/I in isolated mitochondria. (**G**) The effect of paeoniflorin on the viability of U266 myeloma cells. The data are presented as the mean±SD. Every experiment was performed in triplicate. Compared between the control group and the model group**P<0.01, compared between the model group and treated group $^{\Delta}$P<0.05 and $^{\Delta\Delta}$P<0.01.

(P<0.01). Comparison with the model group indicated that the number of the mitochondria-localized LC3 puncta in the cells treated with paeoniflorin was significantly increased, and the relative percentage of the cells with the mitochondria-localized LC3 puncta was significantly increased (Figure 4C, P<0.01). Moreover, bortezomib substantially decreased the colocalization of the lysosomes (labeled with LysoTracker Red) with mitochondria (labeled with MitoTracker Green) (P<0.01). However, paeoniflorin significantly increased the colocalization of the lysosomes and mitochondria after bortezomib treatment of the cells (Figure 4D, P<0.01). Moreover, a decrease in the colocalization of the mitochondria (labeled with MitoTracker Red) with Parkin (green) was observed in the model group (P<0.01). Interestingly, the colocalization of the mitochondria and Parkin in the treated group was significantly higher than that in the model group, and the relative percentage of the cells with colocalization of Parkin and the mitochondria was significantly higher after paeoniflorin treatment (Figure 4E, P<0.01).

Subsequently, we determined whether bortezomib and paeoniflorin plus bortezomib influence the mitochondrial function at the molecular level. The results showed that the levels of the mitochondrial proteins Tim23 and p62 were increased in the model group compared with those in the other groups, and the levels of LC3II/I, beclin-1, and Parkin were significantly reduced (P<0.01). In contrast, the levels of Tim23 and p62 were significantly lower and the levels of LC3II/I, beclin-1, and Parkin were higher than those in the treated group (Figure 4F, P<0.01).

These results indicated that bortezomib induced a decrease in the level of neuronal autophagy, which may be one of the reasons for the occurrence of PN. Paeoniflorin may alleviate BiPN by triggering Parkin-mediated mitochondrial autophagy.

The Effect of Paeoniflorin on U266 Cells Treated with Bortezomib

We designed an experiment to determine whether paeoniflorin interferes with the effect of bortezomib on myeloma cells. The results showed that the viability of the cells of the model group (U266 cells treated with 0.05 μM bortezomib) and treated group (U266 cells treated with 0.05 μM bortezomib + 20 μM paeoniflorin) was significantly decreased at 12 h, 24 h, 36 h, and 48 h compared with that in the control group (untreated U266 cells), (Figure 4G). This finding indicated that paeoniflorin did not alter the therapeutic effect of bortezomib on myeloma cells at the concentration used in this experiment.

Paeoniflorin Effectively Improved the Behavioral Performance of BiPN Model Mice

Mechanical allodynia is a hallmark of BiPN in mice.[35] BiPN was induced in mice by administration of 1 mg/kg bortezomib on days 1, 4, 7, and 11. The protective effect of paeoniflorin on BiPN mice was examined by continuously administering paeoniflorin (50 mg/kg/d) to mice throughout the bortezomib administration period. The results of the cold plate test (Figure 5A) showed that starting from day 4 of the onset of the model, the number of foot lifts in the treated group was significantly reduced compared with that in the model group (P<0.01), suggesting that paeoniflorin effectively improved the behavioral performance of BiPN model mice. A cold plate test was used to assess the hypersensitivity to the cold stimuli. In addition, as shown in Figure 5B, after day 4 of the onset of the model, the number of hind paw licks in the treated group was significantly lower than that in the model group. There were no significant differences between the two groups on days 11 and 16. However, after day 18, a significant difference between the two groups was detected again (Figure 5C, P<0.05 or P<0.01). The results of the thermal paw withdrawal latency test indicated the lack of significant differences in the latency between the treated and model groups in the early stage of the model; however, a significant difference in the thermal paw withdrawal latency was detected in the late stage of the model (after day 18) (P<0.05 or P<0.01), suggesting that paeoniflorin significantly alleviated the thermal sensitivity of BiPN model mice in the late stage of the model.

Paeoniflorin Effectively Ameliorated Sciatic Nerve Damage in BiPN Model Mice

To further characterize sensory neuropathy, we measured the motor nerve conduction velocity (MNCV) of mice every 7 days starting from day 4 after the onset of the model. The MNCV of mice in the model and treated groups was significantly reduced (P<0.05), indicating that the BiPN model was successfully constructed. Extension of paeoniflorin administration time was associated with a gradual increase in the MNCV of mice in the treated group (Figure 5D,

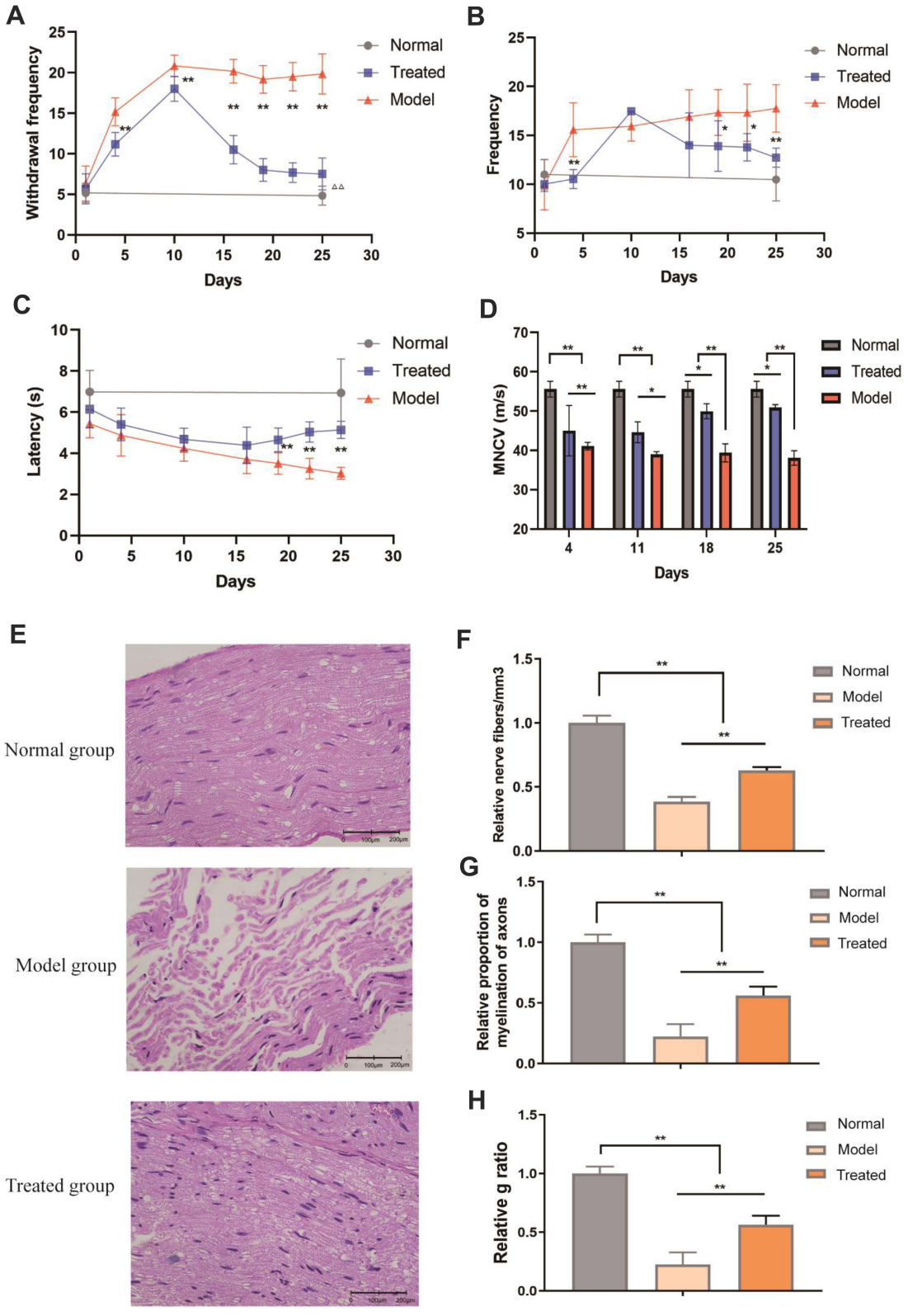

Figure 5 Effects of paeoniflorin on the behavior and sciatic nerve in BiPN mice. (**A**) The results of the cold plate test for each group of mice. (**B**) The results of the hot plate test for each group of mice. (**C**) The thermal paw withdrawal latency for each group of mice. (**D**) The MNCV of each group of mice. (**E**) Morphological changes in the sciatic nerves of mice from each group. (**F**) The relative number of nerve fibers/mm^3 in mice from each group. (**G**) The relative proportion of myelinated axons in each group of mice. (**H**) The g ratio of mice from each group. Each experiment was performed in triplicate. The data are presented as the mean±SD. *P<0.05 and **P<0.01.

P<0.05). The studies of other authors reported a decrease in the nerve conduction velocity in mice treated with bortezomib (BTZ), indicating demyelination that is a sign of nerve damage.[36] The results of our experiments confirmed that paeoniflorin increased the MNCV by reducing nerve damage in mice.

The pathological changes in the sciatic nerves of mice of all groups were assessed on day 25 after the onset of the model (Figure 5E). Imaging of longitudinal sections of the sciatic nerve samples of the normal group showed a tight arrangement of myelinated nerve fibers, normal myelin tissue, and scattered Schwann cells at the edge of the myelin sheath. The sciatic nerves of mice of the treated group were arranged neatly, and some of sciatic nerve fibers were swollen; a small number of the cells lacked their myelin sheath. Sciatic nerve fibers of the model group were disordered and loose, exhibiting inflammatory cell infiltration, fewer sheath cells, some degeneration of the axons, and a few Schwann cells. Subsequently, we quantified the damage to the myelin structure of the sciatic nerve in mice. Comparison with the model group indicated that the relative number of nerve fibers/mm^3, relative proportion of myelination of the axons, and the g ratio were significantly increased in the treated group; these changes reflected the signs of nerve cell recovery (Figure 5F–H, P<0.01).

ROS are physiological and pathological metabolites of the cells that are involved in apoptosis and inflammation. An increase in the level of ROS in a cell often indicates damage to the mitochondria.[37,38] We measured the level of ROS in sciatic nerve cells of BiPN mice. As shown in Figure 6A, after bortezomib treatment, ROS release in the sciatic nerves of mice was significantly increased, and the release of ROS was significantly reduced after paeoniflorin treatment (P<0.01). Electron microscopy images showed that in the model group, the myelin sheath of the sciatic nerve was swollen, the lamella was loose, the edges of the myelin sheath were irregular, and the thickness was uneven; in the treated group, the myelin sheath was dense and complete, and the structural damage was significantly reduced (Figure 6B). These results suggested that paeoniflorin significantly relieved sciatic nerve injury in BiPN model mice.

Paeoniflorin Increased the Level of Autophagy in the Peripheral Nerves of BiPN Model Mice

As shown in Figure 6C, the protein levels of the autophagy-related factors LC3 II/I, Beclin-1, and Parkin were significantly decreased in the model group (P<0.01), and the protein levels of p62 and Tim23 were significantly increased (P<0.01). This result suggested that PN caused by bortezomib may be related to a low level of autophagy in the sciatic nerve and that paeoniflorin enhanced autophagy in the sciatic nerve. Comparison with the model group indicated that the LC3 II/I ratio and the levels of the Beclin-1 and Parkin proteins were significantly increased in the treated group (P<0.01), and the levels of p62 and Tim23 were significantly decreased (P<0.01). We assessed the levels of autophagy-related factors by IHC; comparison with the model group indicated that the expression levels of LC3B and Parkin in the nerve tissue were higher in the treated group ($p < 0.05$), which was consistent with the results of the in vitro experiments (Figure 6D and E). Overall, paeoniflorin significantly alleviated sciatic nerve injury in BiPN mice, and this beneficial effect could have been achieved by reversing a bortezomib-induced decrease in the levels of autophagy.

Discussion

Inflammatory and peripheral immune responses have been reported to be closely associated with CIPN-related pain.[39] Inflammatory factors and peripheral immune factors are aberrantly expressed in damaged nerves and contribute to the development of neuropathic pain.[40,41] The results of the present study in patients receiving bortezomib indicated that BiPN-positive patients had higher plasma IL6 levels than BiPN-negative patients and that the expression level of IL6 was positively correlated with the degree of BiPN. Therefore, we speculated that bortezomib may induce BiPN by interfering with immune balance, leading to increased IL6 levels. Coincidentally, we obtained similar results in the experiments in cultured cells. After bortezomib treatment, the activity of PC12 cells was decreased, and IL6 levels were increased. Interestingly, the results of in vitro experiments indicated that paeoniflorin increased the viability of PC12 cells and decreased the level of IL6 in the cells treated with bortezomib. Paeoniflorin, a water-soluble monoterpene glycoside, is the main bioactive component of *Paeonia lactiflora* Pall.[42] Paeoniflorin has been shown to display a wide spectrum of pharmacological effects, including anti-inflammatory, immunoregulatory,[43] antitumor,[44] and neuroprotective[45,46] effects,

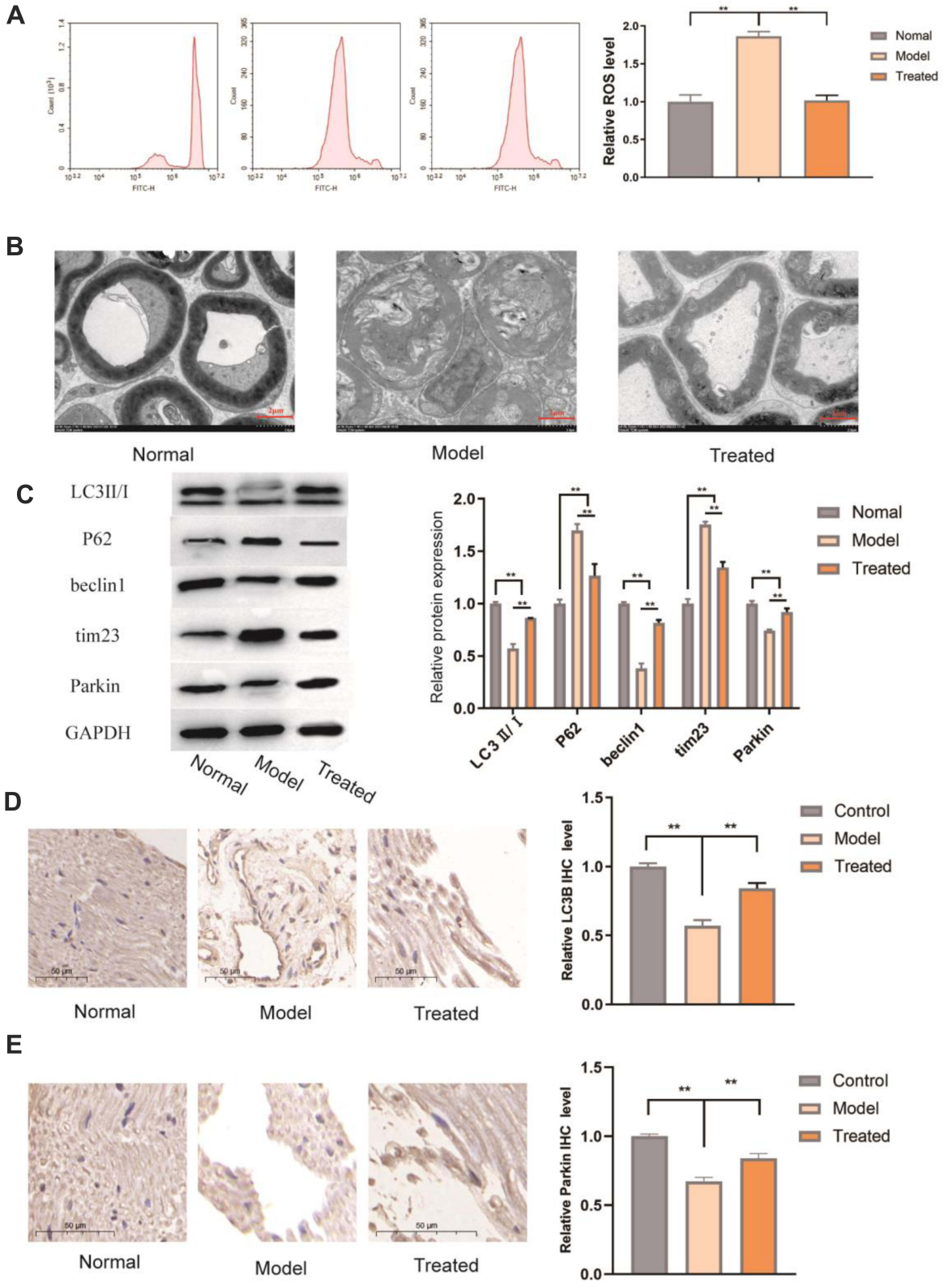

Figure 6 Effects of paeoniflorin on the level of autophagy in the sciatic nerve of BiPN mice. (**A**) ROS levels in various groups. (**B**) The changes in the sciatic nerve myelin structure were detected by electron microscopy in each group of mice. (**C**) WB analysis of the protein levels of PARKIN, p62, Tim23, and LC3II/I in the sciatic nerves of mice of various groups. Each experiment was performed in triplicate. (**D**) Comparison with the model group indicated that the expression of LC3B in the nerve tissues was increased in the treated group. (**E**) Comparison with the model group indicated that the expression of Parkin was increased in the nerve tissues in the treated group. The data are presented as the mean±SD. **P<0.01.

which emphasize potential therapeutic efficacy of paeoniflorin. The data of network pharmacology analysis indicated that various targets, such as TNF, TP53, AKT1, and IL6, were closely associated with the effect of paeoniflorin on PN. The data of GO and KEGG analyses also showed that paeoniflorin may be able to regulate nerve-related proliferation and autophagy-related and inflammatory biological processes to influence the growth of nerve cells. These findings demonstrated the potential of paeoniflorin as a treatment for PN. However, these targets were identified by computational analysis, and the results had to be verified in animal experiments.

Mitochondrial dysfunction is a key factor in the occurrence of PN.[47,48] Many studies have confirmed that autophagy disorders are closely related to the occurrence of PN. Promotion of peripheral nerve autophagy is able to reduce mitochondrial dysfunction and the level of apoptosis to relieve CIPN.[49] In addition, promoting autophagy in Schwann cells helps reduce protein aggregation and alleviates BiPN.[50] IL6 has been reported to be closely related to autophagy. Takagaki et al[51] have demonstrated that the lack of autophagy in endothelial cells induces IL6 synthesis/secretion. However, IL6 has been reported to promote autophagy in many types of cancer. The role of IL6 in autophagy remains controversial, and specific effects may depend on cellular microenvironment.[52,53] Parkin is an E3 ubiquitin ligase that can trigger mitochondrial autophagy by degrading outer mitochondrial membrane proteins and is considered the core factor of the mitochondrial autophagy pathway.[54,55] Additionally, Parkin plays an important role in maintaining the survival of the neurons. Parkin reduces the damaging effect of neurotoxins and metal ions on the nerves.[56] During autophagy, LC3 is converted from the cytosolic LC3-I form to the membrane-bound LC3-II form, which is lipidated and accumulates on the autophagosome membrane. The autophagosome fuses with the lysosome to form an autophagolysosome, which is then broken down. The ubiquitin-related protein p62, which binds to LC3, is also used to monitor the autophagic flux.[57] PC12 cells are derived from rat pheochromocytoma cells and are widely used for neurotoxicity assessment.[58] The present study analyzed the toxic effects of bortezomib on PC12-derived neuronal cells. After bortezomib treatment, the activity of PC12 cells was significantly reduced, the level of autophagy was decreased, the mitochondria were significantly damaged, and IL6 levels were significantly elevated. Paeoniflorin significantly reduced bortezomib-induced damage to the mitochondria of PC12 cells and relieved mitochondrial energy imbalance. After administration of paeoniflorin, NAO levels were restored to normal levels, the apoptosis rate of the cells was decreased, the expression of the p62 and Tim23 proteins was decreased, and the expression of the LC3II, beclin-1, and Parkin proteins was increased. This finding indicated that paeoniflorin significantly reduced bortezomib-induced damage to PC12 cells and that the mechanism of this effect may be related to the regulation of the Parkin-mediated mitochondrial autophagy pathway.

Paeoniflorin has been shown to significantly alleviate PN caused by diabetes and paclitaxel.[24,59,60] The present study is the first to report the protective effect of paeoniflorin on bortezomib-induced peripheral neuropathy. In the present study, bortezomib was used to induce peripheral neuropathy in C57BL/6J mice, and the effects of paeoniflorin on inflammation and autophagy were investigated in a model of peripheral neuropathy. The data indicated that intraperitoneal injection of bortezomib (1 mg/kg, days 1, 4, 8, and 11) induced PN in mice. Bortezomib promoted the production of the proinflammatory cytokine IL6 in mice and reduced the levels of autophagy in the mouse sciatic nerve. Paeoniflorin ameliorated peripheral neuropathy in BiPN model mice and protected the sciatic nerve from bortezomib-mediated damage, possibly acting by reducing the level of inflammation, increasing the level of autophagy, and maintaining mitochondrial homeostasis.

We assessed neuropathy in bortezomib-treated mice by evaluating mechanical allodynia, thermal hyperalgesia, and conduction velocity.[57] As expected, mice clearly manifested mechanical allodynia after the administration of bortezomib, and paeoniflorin significantly reduced the occurrence of pain and mechanical hypersensitivity. Subsequent monitoring of the changes in the motor nerve conduction velocity and nerve tissue structure in BiPN model mice demonstrated that paeoniflorin significantly increased the motor nerve conduction velocity and reduced the damage to the myelin structure of the sciatic nerve in BiPN model mice. After paeoniflorin treatment, the level of autophagy in the sciatic nerve cells of BiPN model mice was increased, ROS release was decreased, the expression of LC3II/I, Beclin-1, and Parkin was significantly increased, and the expression of p62 and Tim23 was reduced. LC3 isoform B (LC3B) is one of the most commonly used markers of autophagy. The data of immunohistochemistry showed that paeoniflorin significantly increased the expression of LC3B and Parkin in the sciatic nerves of BiPN model mice. These results suggested that bortezomib-induced peripheral neurotoxicity in mice was associated with inflammation, impairment of autophagy, oxidative stress, and mitochondrial damage and that paeoniflorin reduced

BiPN-mediated damage by reversing the changes in these pathways. The results of the experiments with cultured cells also showed that paeoniflorin reduced the level of IL6 in PC12 cells after bortezomib treatment, increased the level of autophagy, and reduce bortezomib-induced damage to these cells. Therefore, our conclusions were similar based on the results of in vivo and in vitro studies. At present, we have verified only the protective effect of paeoniflorin, which may be due to counteracting neuroinflammation and reducing autophagy injury. Further experiments are needed to confirm the long-term therapeutic effect of paeoniflorin in BiPN.

Conclusion

The present study confirmed that paeoniflorin significantly alleviated peripheral neuropathy caused by bortezomib, possibly by reducing IL6 levels to regulate PARKIN-mediated mitochondrial autophagy and mitochondrial damage. Paeoniflorin is an effective agent for the treatment of BiPN; however, further investigations are needed.

Abbreviations

BiPN, bortezomib-induced peripheral neuropathy; MM, multiple myeloma; IL6, interleukin-6; HE, hematoxylin-eosin; ROS, reactive oxygen species; IHC, immunohistochemistry; PN, peripheral neuropathy; CIPN, chemotherapy-induced peripheral neuropathy; TNF-α, tumor necrosis factor alpha; mtDNA, mitochondrial DNA; ELISA, enzyme-linked immunosorbent assay; NCI-CTCAE, National Cancer Institute Common Toxicity Criteria for Adverse Events; CCK-8, Cell Counting Kit-8; NAO, 10-N-nonyl acridine orange; GO, Gene Ontology; KEGG, Kyoto Encyclopedia of Genes and Genomes; FBS, fetal bovine serum; MAO, monoamine oxidase; COX, cyclooxygenase; HPLC, high-performance liquid chromatography; BCA, bicinchoninic acid; PVDF, polyvinylidene difluoride; MNCV, motor nerve conduction velocity; DAB, diaminobenzidine; ROC, receiver operating characteristic; DCFDA, dichlorofluorescin diacetate.

Data Sharing Statement

The datasets generated and/or analyzed during the current study are not publicly available because the data are confidential; however, the data are available from the corresponding author upon reasonable request.

Ethics Approval and Consent to Participate

All experimental methods were approved by the Ethics Committee of the Affiliated Hospital of Shandong University of Traditional Chinese Medicine.

Author Contributions

All authors made significant contributions to the conception and design, acquisition of data, or analysis and interpretation of data; took part in drafting the article or revising it critically for important intellectual content (including network pharmacology and in vivo and in vitro experiments); agreed to submit to the current journal; gave final approval of the version to be published; and agree to be accountable for all aspects of the work.

Funding

The present work was supported by the National Natural Science Foundation of China (no. 82074348), the Taishan Scholar Project (tsqn201812145), the Key Technology Research and Development Program of Shandong (no. 2019GSF108162), and the Natural Science Foundation of Shandong Province (no. ZR2020MH388).

Disclosure

All authors declare that there are no conflicts of interest.

References

1. De Raeve HR, Vanderkerken K. The role of the bone marrow microenvironment in multiple myeloma. *Histol Histopathol*. 2005;20(4):1227–1250. doi:10.14670/HH-20.1227

2. Mateos MV, San Miguel JF. Management of multiple myeloma in the newly diagnosed patient. *Hematology Am Soc Hematol Educ Program*. 2017;2017(1):498–507. doi:10.1182/asheducation-2017.1.498
3. Yamamoto S, Egashira N. Pathological mechanisms of bortezomib-induced peripheral neuropathy. *Int J Mol Sci*. 2021;22(2):888. doi:10.3390/ijms22020888
4. Xu Y, Xing L, Su J, et al. Model-based clustering for identifying disease-associated SNPs in case-control genome-wide association studies. *Sci Rep*. 2019;9(1):13686. doi:10.1038/s41598-019-50229-6
5. Dimopoulos MA, Mateos MV, Richardson PG, et al. Risk factors for, and reversibility of, peripheral neuropathy associated with bortezomib-melphalan-prednisone in newly diagnosed patients with multiple myeloma: subanalysis of the Phase 3 Vista study. *Eur J Haematol*. 2011;86(1):23–31. doi:10.1111/j.1600-0609.2010.01533.x
6. Meregalli C, Maricich Y, Cavaletti G, et al. Reversal of bortezomib-induced neurotoxicity by suvecaltamide, a selective T-type Ca-channel modulator, in preclinical models. *Cancers*. 2021;13(19):5013. doi:10.3390/cancers13195013
7. Łuczkowska K, Rogińska D, Kulig P, et al. Bortezomib-induced epigenetic alterations in nerve cells: focus on the mechanisms contributing to the peripheral neuropathy development. *Int J Mol Sci*. 2022;23(5):2431. doi:10.3390/ijms23052431
8. Maharjan S, Oku M, Tsuda M, et al. Mitochondrial impairment triggers cytosolic oxidative stress and cell death following proteasome inhibition. *Sci Rep*. 2014;4:5896. doi:10.1038/srep05896
9. Trecarichi A, Flatters SJL. Mitochondrial dysfunction in the pathogenesis of chemotherapy-induced peripheral neuropathy. *Int Rev Neurobiol*. 2019;145:83–126. doi:10.1016/bs.irn.2019.05.001
10. Yin Y, Qi X, Qiao Y, et al. The association of neuronal stress with activating transcription factor 3 in dorsal root ganglion of in vivo and in vitro models of bortezomib-induced neuropathy. *Curr Cancer Drug Targets*. 2019;19(1):50–64. doi:10.2174/1568009618666181003170027
11. Cavaletti G, Gilardini A, Canta A, et al. Bortezomib-induced peripheral neurotoxicity: a neurophysiological and pathological study in the rat. *Exp Neurol*. 2007;204(1):317–325. doi:10.1016/j.expneurol.2006.11.010
12. Janes K, Doyle T, Bryant L, et al. Bioenergetic deficits in peripheral nerve sensory axons during chemotherapy-induced neuropathic pain resulting from peroxynitrite-mediated post-translational nitration of mitochondrial superoxide dismutase. *Pain*. 2013;154(11):2432–2440. doi:10.1016/j.pain.2013.07.032
13. Sabirzhanov B, Li Y, Coll-Miro M, et al. Inhibition of NOX2 signaling limits pain-related behavior and improves motor function in male mice after spinal cord injury: participation of IL-10/miR-155 pathways. *Brain Behav Immun*. 2019;80:73–87. doi:10.1016/j.bbi.2019.02.024
14. Lees JG, Makker PG, Tonkin RS, et al. Immune-mediated processes implicated in chemotherapy-induced peripheral neuropathy. *Eur J Cancer*. 2017;73:22–29. doi:10.1016/j.ejca.2016.12.006
15. Alé A, Bruna J, Morell M, et al. Treatment with anti-TNF alpha protects against the neuropathy induced by the proteasome inhibitor bortezomib in a mouse model. *Exp Neurol*. 2014;253:165–173. doi:10.1016/j.expneurol.2013.12.020
16. Mangiacavalli S, Corso A, De Amici M, et al. Emergent T-helper 2 profile with high interleukin-6 levels correlates with the appearance of bortezomib-induced neuropathic pain. *Br J Haematol*. 2010;149(6):916–918. doi:10.1111/j.1365-2141.2010.08138.x
17. Yang H, Liu C, Yuan F, et al. Clinical significance of SIRT3 and inflammatory factors in multiple myeloma patients with bortezomib-induced peripheral neuropathy: a cohort study. *Scand J Clin Lab Invest*. 2021;81(8):615–621. doi:10.1080/00365513.2021.1986857
18. Guo Y, Xu X, Huang J, et al. The actions and mechanisms of P2X7R and p38 MAPK activation in mediating bortezomib-induced neuropathic pain. *Biomed Res Int*. 2020;2020:8143754. doi:10.1155/2020/8143754
19. Zhang Q, Zhou J, Shen M, et al. Pyrroloquinoline quinone inhibits rotenone-induced microglia inflammation by enhancing autophagy. *Molecules*. 2020;25(19):4359. doi:10.3390/molecules25194359
20. Borsche M, König IR, Delcambre S, et al. Mitochondrial damage-associated inflammation highlights biomarkers in PRKN/PINK1 parkinsonism. *Brain*. 2020;143(10):3041–3051. doi:10.1093/brain/awaa246
21. Sliter DA, Martinez J, Hao L, et al. Parkin and PINK1 mitigate STING-induced inflammation. *Nature*. 2018;561(7722):258–262. doi:10.1038/s41586-018-0448-9
22. Tyrrell DJ, Blin MG, Song J, et al. Aging impairs mitochondrial function and mitophagy and elevates interleukin 6 within the cerebral vasculature. *J Am Heart Assoc*. 2020;9(23):e017820. doi:10.1161/JAHA.120.017820
23. Tu J, Guo Y, Hong W, et al. The regulatory effects of paeoniflorin and its derivative paeoniflorin-6'-O-benzene sulfonate CP-25 on inflammation and immune diseases. *Front Pharmacol*. 2019;10:57. doi:10.3389/fphar.2019.00057
24. Liu P, Cheng J, Ma S, et al. Paeoniflorin attenuates chronic constriction injury-induced neuropathic pain by suppressing spinal NLRP3 inflammasome activation. *Inflammopharmacology*. 2020;28(6):1495–1508. doi:10.1007/s10787-020-00737-z
25. Yu X, Man R, Li Y, et al. Paeoniflorin protects spiral ganglion neurons from cisplatin-induced ototoxicity: possible relation to PINK1/BAD pathway. *J Cell Mol Med*. 2019;23(8):5098–5107. doi:10.1111/jcmm.14379
26. Tang H, Wu L, Chen X, et al. Paeoniflorin improves functional recovery through repressing neuroinflammation and facilitating neurogenesis in rat stroke model. *PeerJ*. 2021;9:e10921. doi:10.7717/peerj.10921
27. Ma XH, Duan WJ, Mo YS, et al. Neuroprotective effect of paeoniflorin on okadaic acid-induced tau hyperphosphorylation via calpain/Akt/GSK-3β pathway in SH-SY5Y cells. *Brain Res*. 2018;1690:1–11. doi:10.1016/j.brainres.2018.03.022
28. Toyama S, Shimoyama N, Szeto HH, et al. Protective effect of a mitochondria-targeted peptide against the development of chemotherapy-induced peripheral neuropathy in mice. *ACS Chem Neurosci*. 2018;9(7):1566–1571. doi:10.1021/acschemneuro.8b00013
29. Vachon P, Millecamps M, Low L, et al. Alleviation of chronic neuropathic pain by environmental enrichment in mice well after the establishment of chronic pain. *Behav Brain Funct*. 2013;9:22. doi:10.1186/1744-9081-9-22
30. Duggett NA, Flatters SJL. Characterization of a rat model of bortezomib-induced painful neuropathy. *Br J Pharmacol*. 2017;174(24):4812–4825. doi:10.1111/bph.14063
31. Walsh ME, Sloane LB, Fischer KE, et al. Use of nerve conduction velocity to assess peripheral nerve health in aging mice. *J Gerontol a Biol Sci Med Sci*. 2015;70(11):1312–1319. doi:10.1093/gerona/glu208
32. Shinouchi R, Shibata K, Hashimoto T, et al. SMTP-44D improves diabetic neuropathy symptoms in mice through its antioxidant and anti-inflammatory activities. *Pharmacol Res Perspect*. 2020;8(6):e00648. doi:10.1002/prp2.648
33. Jacobson J, Duchen MR, Heales SJ. Intracellular distribution of the fluorescent dye nonyl acridine Orange responds to the mitochondrial membrane potential: implications for assays of cardiolipin and mitochondrial mass. *J Neurochem*. 2002;82(2):224–233. doi:10.1046/j.1471-4159.2002.00945.x

34. Deramchia K, Morand P, Biran M, et al. Contribution of pyruvate phosphate dikinase in the maintenance of the glycosomal ATP/ADP balance in the Trypanosoma brucei procyclic form. *J Biol Chem*. 2014;289(25):17365–17378. doi:10.1074/jbc.M114.567230
35. Authier N, Balayssac D, Marchand F, et al. Animal models of chemotherapy-evoked painful peripheral neuropathies. *Neurotherapeutics*. 2009;6 (4):620–629. doi:10.1016/j.nurt.2009.07.003
36. Meregalli C, Marjanovic I, Scali C, et al. High-dose intravenous immunoglobulins reduce nerve macrophage infiltration and the severity of bortezomib-induced peripheral neurotoxicity in rats. *J Neuroinflammation*. 2018;15(1):232. doi:10.1186/s12974-018-1270-x
37. Dhupal M, Oh JM, Tripathy DR, et al. Immunotoxicity of titanium dioxide nanoparticles via simultaneous induction of apoptosis and multiple toll-like receptors signaling through ROS-dependent SAPK/JNK and p38 MAPK activation. *Int J Nanomedicine*. 2018;23(13):6735–6750. doi:10.2147/IJN.S176087
38. Badrinath N, Yoo SY. Mitochondria in cancer: in the aspects of tumorigenesis and targeted therapy. *Carcinogenesis*. 2018;39(12):1419–1430. doi:10.1093/carcin/bgy148
39. Suo J, Wang M, Zhang P, et al. Siwei Jianbu decoction improves painful paclitaxel-induced peripheral neuropathy in mouse model by modulating the NF-κB and MAPK signaling pathways. *Regen Med Res*. 2020;8:2. doi:10.1051/rmr/200001
40. Hu Z, Deng N, Liu K, et al. CNTF-STAT3-IL-6 axis mediates neuroinflammatory cascade across Schwann cell-neuron-microglia. *Cell Rep*. 2020;31(7):107657. doi:10.1016/j.celrep.2020.107657
41. Magrinelli F, Briani C, Romano M, et al. The association between serum cytokines and damage to large and small nerve fibers in diabetic peripheral neuropathy. *J Diabetes Res*. 2015;2015:547834. doi:10.1155/2015/547834
42. Zhou YX, Gong XH, Zhang H, et al. A review on the pharmacokinetics of paeoniflorin and its anti-inflammatory and immunomodulatory effects. *Biomed Pharmacother*. 2020;130:110505. doi:10.1016/j.biopha.2020.110505
43. Chen T, Guo ZP, Jiao XY, et al. Protective effects of peoniflorin against hydrogen peroxide-induced oxidative stress in human umbilical vein endothelial cells. *Can J Physiol Pharmacol*. 2011;89(6):445–453. doi:10.1139/y11-034
44. Xiang Y, Zhang Q, Wei S, et al. Paeoniflorin: a monoterpene glycoside from plants of Paeoniaceae family with diverse anticancer activities. *J Pharm Pharmacol*. 2020;72(4):483–495. doi:10.1111/jphp.13204
45. Wang B, Dai W, Shi L, et al. Neuroprotection by paeoniflorin against nuclear factor kappa B-induced neuroinflammation on spinal cord injury. *Biomed Res Int*. 2018;2018:9865403. doi:10.1155/2018/9865403
46. Zheng M, Liu C, Fan Y, et al. Neuroprotection by Paeoniflorin in the MPTP mouse model of Parkinson's disease. *Neuropharmacology*. 2017;116:412–420. doi:10.1016/j.neuropharm.2017.01.009
47. Areti A, Komirishetty P, Kalvala AK, et al. Rosmarinic acid mitigates mitochondrial dysfunction and spinal glial activation in oxaliplatin-induced peripheral neuropathy. *Mol Neurobiol*. 2018;55(9):7463–7475. doi:10.1007/s12035-018-0920-4
48. Yang Y, Luo L, Cai X, et al. Nrf2 inhibits oxaliplatin-induced peripheral neuropathy via protection of mitochondrial function. *Free Radic Biol Med*. 2018;120:13–24. doi:10.1016/j.freeradbiomed.2018.03.007
49. Areti A, Komirishetty P, Akuthota M, et al. Melatonin prevents mitochondrial dysfunction and promotes neuroprotection by inducing autophagy during oxaliplatin-evoked peripheral neuropathy. *J Pineal Res*. 2017;62(3):e12393. doi:10.1111/jpi.12393
50. Watanabe T, Nagase K, Chosa M, et al. Schwann cell autophagy induced by SAHA, 17-AAG, or clonazepam can reduce bortezomib-induced peripheral neuropathy. *Br J Cancer*. 2010;103(10):1580–1587. doi:10.1038/sj.bjc.6605954
51. Takagaki Y, Lee SM, Dongqing Z, et al. Endothelial autophagy deficiency induces IL6 - dependent endothelial mesenchymal transition and organ fibrosis. *Autophagy*. 2020;16(10):1905–1914. doi:10.1080/15548627.2020.1713641
52. Katheder NS, Khezri R, O'Farrell F, et al. Microenvironmental autophagy promotes tumour growth. *Nature*. 2017;541(7637):417–420. doi:10.1038/nature20815
53. Nogueira-Recalde U, Lorenzo-Gómez I, Blanco FJ, et al. Fibrates as drugs with senolytic and autophagic activity for osteoarthritis therapy. *EBioMedicine*. 2019;45:588–605. doi:10.1016/j.ebiom.2019.06.049
54. Pickrell AM, Youle RJ. The roles of PINK1, parkin, and mitochondrial fidelity in Parkinson's disease. *Neuron*. 2015;85(2):257–273. doi:10.1016/j.neuron.2014.12.007
55. Miller S, Muqit MMK. Therapeutic approaches to enhance PINK1/Parkin mediated mitophagy for the treatment of Parkinson's disease. *Neurosci Lett*. 2019;705:7–13. doi:10.1016/j.neulet.2019.04.029
56. Kubo S, Hatano T, Takanashi M, et al. Can parkin be a target for future treatment of Parkinson's disease? *Expert Opin Ther Targets*. 2013;17 (10):1133–1144. doi:10.1517/14728222.2013.827173
57. Liu CC, Huang ZX, Li X, et al. Upregulation of NLRP3 via STAT3-dependent histone acetylation contributes to painful neuropathy induced by bortezomib. *Exp Neurol*. 2018;302:104–111. doi:10.1016/j.expneurol.2018.01.011
58. Piwowar A, Rembiałkowska N, Rorbach-Dolata A, et al. Anemarrhenae asphodeloides rhizoma extract enriched in mangiferin protects PC12 cells against a neurotoxic agent-3-nitropropionic acid. *Int J Mol Sci*. 2020;21(7):2510. doi:10.3390/ijms21072510
59. Andoh T, Kobayashi N, Uta D, et al. Prophylactic topical paeoniflorin prevents mechanical allodynia caused by paclitaxel in mice through adenosine A1 receptors. *Phytomedicine*. 2017;25:1–7. doi:10.1016/j.phymed.2016.12.010
60. Zhu Y, Han S, Li X, et al. Paeoniflorin effect of Schwann cell-derived exosomes ameliorates dorsal root ganglion neurons apoptosis through IRE1α pathway. *Evid Based Complement Alternat Med*. 2021;2021:6079305. doi:10.1155/2021/6079305